JOURNAL OF ELECTROMAGNETIC ENGINEERING AND SCIENCE, VOL. 16, NO. 3, 150~158, JUL. 2016

http://dx.doi.org/10.5515/JKIEES.2016.16.3.150
ISSN 2234-8395 (Online) · ISSN 2234-8409 (Print)

Effects of Sheet Thickness on the Electromagnetic Wave Absorbing Characterization of $Li_{0.375}Ni_{0.375}Zn_{0.25}$-Ferrite Composite as a Radiation Absorbent Material

Dong-Young Kim[1*] · Young-Ho Yoon[1] · Kwan-Jun Jo[1] · Gil-Bong Jung[1] · Chong-Chul An[2]

Abstract

This paper reports on a study of LiNiZn-ferrite composite as a radiation absorbent material (RAM). The electromagnetic (EM) wave absorbers are composed of an EM wave absorbing material and a polymeric binder. The surface morphology, chemical composition, weight percent of the ferrite composite of the toroid sample, magnetic properties, and return loss are investigated using field emission scanning electron microscopy (FE-SEM), energy dispersive X-ray spectroscopy (EDX), X-ray photoelectron spectroscopy (XPS), thermogravimetric analysis (TGA), vibrating sample magnetometer (VSM), and network analyzer. For preparing the absorbing sheet, chlorinated polyethylene (CPE) is used as a polymeric binder. The EM wave absorption properties of the prepared samples were studied at 4 − 8 GHz. We can confirm the effects of the thickness of the samples for absorption properties. An absorption bandwidth of more than a 10-dB return loss shifts toward a lower frequency range along with an increase in the thickness of the absorber.

Key Words: Electromagnetic Wave Absorber, Ferrite Composite, LiNiZn-Ferrite, Return Loss.

I. INTRODUCTION

In recent years, the problems of electromagnetic interference (EMI) and electromagnetic susceptibility (EMS) have become more serious due to the wide application of electromagnetic (EM) wave in the GHz range for mobile phones, local area networks, radar systems, and so on. The problems are a malfunction of precise electronic equipment and leak of secret information occurred by a leakage of EM wave. For example, radar systems create false images in the radar because of false echoes. The false echoes are caused by reflection of radar beam from ship's structures such as a mast. When such reflection occurs, the false echoes will return from a legitimate radar contact to antenna by indirect paths. Consequently, the false echoes will make false images appear on the display. Because false echoes cause navigating hazards, EM wave absorbers should be used to cover ship's structures such as a mast [1–5]. At present, EM wave absorbers fabricated in the form of sheets by mixing polymer with absorbent powder have become the focus of current studies, because of their practical and simple preparation method. To our knowledge, ferrites might be a candidate as an EM wave absorbing material because of their high specific resistance, remarkable flexibility in tailoring magnetic properties, and ease of preparation. In past decades, spinel ferrites were utilized as the most common absorbing materials in various forms. Among the EM wave absorbing materials, ferrite was most studied in experiments and applied in both military and civil fields because of its large saturation magnetization, anti-

Manuscript received March 9, 2016 ; Revised June 13, 2016 ; Accepted June 14, 2016. (ID No. 20160309-009J)
[1]Defense Agency for Technology and Quality, Ulsan, Korea.
[2]MA Electronic Co., Cheonan, Korea.
[*]Corresponding Author: Dong-Young Kim (e-mail: intellab@naver.com)

oxidation, and corrosion resistance [6–9]. In previous studies, among the spinel ferrites, LiZn-ferrite and NiZn-ferrite have been used in EM wave absorber materials in VHF and UHF bands [10–15]. In this study, as an absorbent material, ferrite composite was composed of lithium, nickel, and zinc. The EM wave absorption properties of the prepared samples were studied at 4–8 GHz and were determined at different frequencies and sample thicknesses.

II. PREPARATION OF FERRITE COMPOSITE SAMPLE

The ferrite composite was synthesized by ceramic route. The raw materials were lithium carbonate (Li_2CO_3; Samchun Chemical, Seoul, Korea), nickel(II) oxide (NiO; Samchun), zinc oxide (ZnO; Samchun), and iron(III) oxide (Fe_2O_3; Samchun). The starting powders of Li_2CO_3, NiO, ZnO, and Fe_2O_3 were mixed together. Their cationic molar ratios were adjusted to the stoichiometric compositions: $Li_{0.375}Ni_{0.375}Zn_{0.25}$-ferrite. The mixture was calcinated and sintered in a furnace [10–12, 16].

We prepared chlorinated polyethylene (CPE) as a polymeric binder. The two-roll mill was used to mix the ferrite composite with CPE. The weight percent ratio of ferrite composite to polymeric binder was 75:25. The thicknesses of the samples were 1, 2, 4, 6, and 8 mm. For the investigation of the EM wave absorption properties, the prepared composite absorbers were cut into a cylindrical toroid shape with an outer diameter of 20 mm and an inner diameter of 9 mm. Fig. 1 shows the structure of the proposed EM wave absorber [7–9].

A field emission scanning electron microscopy (FE-SEM; JSM-6500F, JEOL Ltd., Tokyo, Japan) was equipped with an energy dispersive X-ray spectroscopy (EDX). FE-SEM was used to analyze the surface morphology, while an EDX analysis was performed to analyze elemental constituents on the surface of sample [17, 18]. X-ray photoelectron spectroscopy (XPS; K-Alpha, Thermo Scientific, Waltham, MA, USA) was used to analyze the elemental constituents on the surface of the sample through the detection of electron binding energy. After the two-roll mill was used to mix the ferrite composite with CPE, the weight percent ratio of ferrite composite to CPE at the sample was compared with the experimental design using a thermogravimetric analysis (TGA; STA409C, Netzsch, Selb, Germany). TGA was performed at a heating rate of 10°C/min in nitrogen [19]. The magnetic properties were evaluated on a vibrating sample magnetometer (VSM; Lake Shore Cryotronics Inc., Westerville, OH, USA) and the magnetic field reached up to 10 kOe.VSM was used to determine the hysteresis curve of the ferrite composite at room temperature [17, 20, 21]. To prepare the measurement of the return loss, the toroid samples were inserted into the coaxial sample holder. The variations in the return loss versus frequency in the range of 10 MHz to 12 GHz were investigated using a network analyzer(Agilent E8363B; Agilent Technologies, Santa Clara, CA, USA) [22–24].

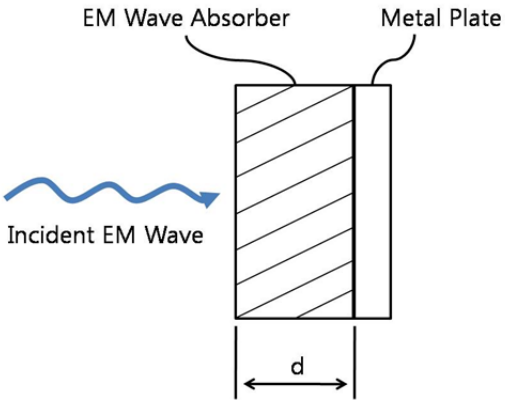

Fig. 1. Structure of proposed EM wave absorber.

III. RESULTS AND DISCUSSIONS

Fig. 2(a) and (b) show the SEM images of Fe_2O_3 particles without heat treatment. Fig. 3(a) and (b) show the SEM images of LiNiZn-ferrite particles with heat treatment. Figs. 2(b) and 3(b) are the magnified views of SEM images. In Fig. 2(b), the appearances of particles are irregular fragment shapes and the surfaces of the particles are rough. In Fig. 3(b), the appearances of particles are spherical in shape and the surfaces of particles are smooth when Fig. 3(b) is compared with Fig. 2(b). It is determined that the lithium oxide, nickel oxide, zinc oxide, and iron oxide particles were mixed and agglomerated to make LiNiZn-ferrite particles [24].

The SEM image and EDX spectrum of LiNiZn-ferrite particles are presented in Fig. 4(a) and (b). On the surface of the particle, the elemental concentrations determined by EDX are displayed in Table 1. The weight percents of nickel and zinc are 5.22% and 13.06%, respectively. It is determined that the weight percents of elements are derived from oxide compounds and heat treatment. It is clear that LiNiZn-ferrite particles consist of iron, nickel, and zinc elements.

Table 1. Elemental concentrations determined by EDX on the surface of LiNiZn-ferrite particle

Element	Weight %	Atomic %
OK	45.51	75.22
FeK	36.21	17.15
NiK	5.22	2.35
ZnL	13.06	5.28

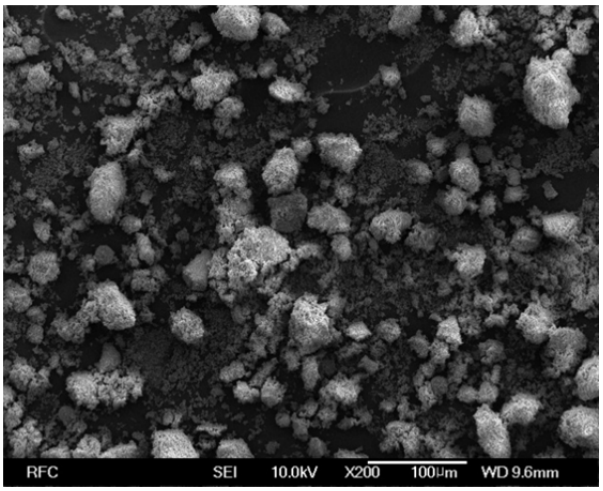

(a)

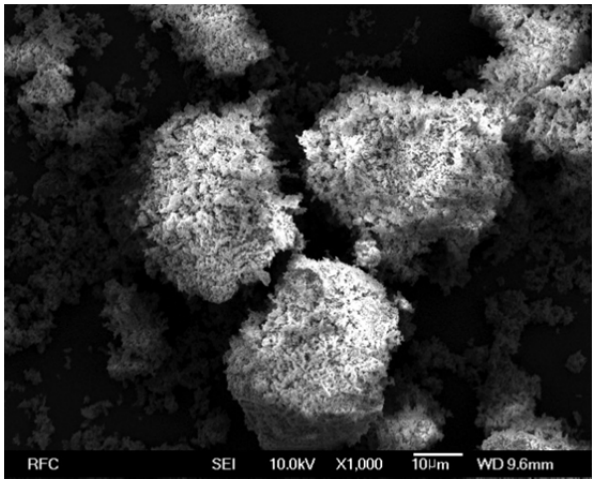

(b)

Fig. 2. SEM images of Fe_2O_3 particles: (a) ×200, (b) ×1,000.

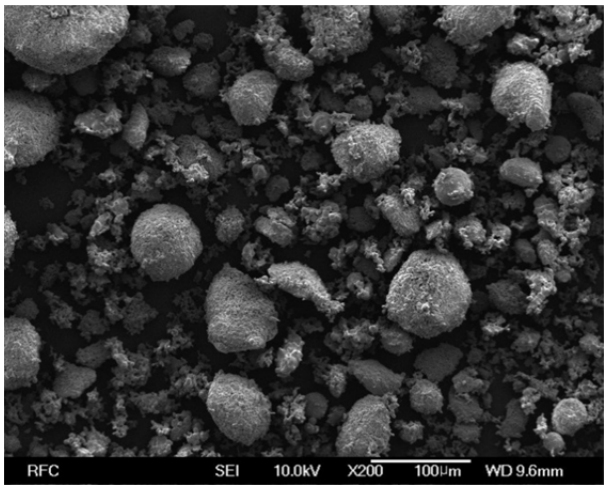

(a)

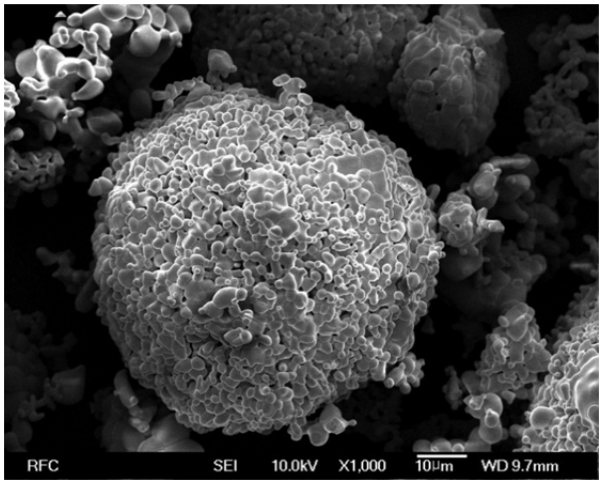

(b)

Fig. 3. SEM images of LiNiZn-ferrite particles: (a) ×200, (b) ×1,000.

However, lithium could not be detected by EDX, as the electrons of lithium are located at a low energy level. The dispersions of elements are presented in Fig. 5(a)–(e) [17, 18].

XPS is a surface-sensitive quantitative spectroscopic technique that measures the elemental composition at the parts per thousand ranges, the empirical formula, the chemical state, and the electronic state of the elements that exist within a material.

A typical XPS spectrum is a plot of the number of electrons detected (sometimes per unit time; Y-axis, ordinate) versus the binding energy of the electrons detected (X-axis, abscissa). Each element produces a characteristic set of XPS peaks at characteristic binding energy values that directly identify each element that exists in or on the surface of the material being analyzed. These characteristic spectral peaks correspond to the electron configuration of the electrons within the atoms, e.g., 1s, 2s, 2p, 3s, etc.

XPS counts electrons ejected from a sample surface when irradiated by X-rays. A spectrum representing the number of electrons recorded at a sequence of energies includes both a contribution from a background signal and resonance peaks characteristic of the bound states of the electrons in the surface atoms.

The resonance peaks above the background are the significant features in an XPS spectrum. For the most part, XPS spectra are quantified in terms of peak intensities and peak positions. The peak intensities measure how much of a material is at the surface, while the peak positions indicate the elemental and chemical compositions. Other values, such as the full width at half maximum (FWHM) are useful indicators of chemical state changes and physical influences. That is, the broadening of a peak may indicate: a change in the number of chemical bonds contributing to a peak shape, a change in the sample condition (X-ray damage), and differential charging of the surface (localized differences in the charge state of the surface). The XPS spectrum of the elements on the surface of LiNiZn-ferrite is shown in Fig. 6. On the surface of the sample, the peak posi-

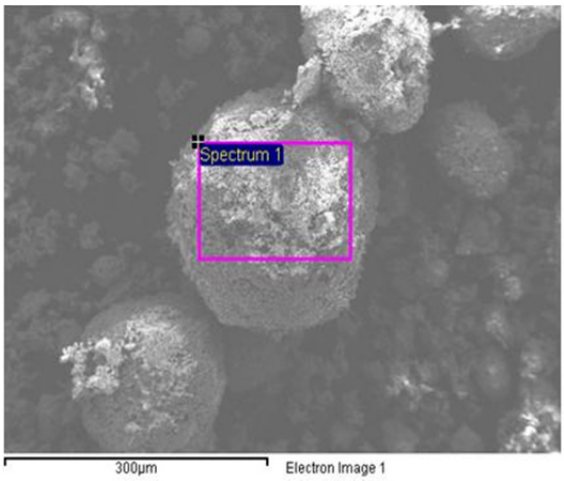

(a)

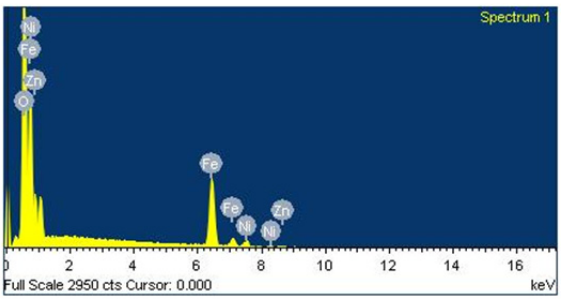

(b)

Fig. 4. SEM image (a) and EDX spectrum (b) of LiNiZn-ferrite particles.

tions and the FWHM of the peaks determined by XPS are displayed in Table 2. In Fig. 7(a), the Li 1s peak position of lithium is approximately at 55.90 eV and the FWHM of the Li 1s peak is 3.49 eV. The Li 1s peak consists of Li_2CO_3 and lithium carbide. In Fig. 7(b), the C 1s peak position of carbon is approximately at 284.55 eV and the FWHM of the C 1s peak is 2.04 eV. The C 1s peak consists of O–C = O, carbonate, C–O–C, C–C, and carbide. In Fig. 7(c), the O 1s peak position of oxygen is approximately at 529.97 eV and the FWHM of the O 1s peak is 3.99 eV. The O 1s peak consists of C–O–C, O–C = O, metal CO_3, and metal oxide. In Fig. 7(d), the Fe 2p peak position of iron is approximately at 710.77 eV and the FWHM

Table 2. Peak positions and FWHM of peaks determined by XPS on the surface of LiNiZn-ferrite particle

Element	Peak BE	FWHM eV
Li 1s	55.90	3.49
Zn 2p	1,020.29	3.33
O 1s	529.97	3.99
Ni 2p	854.24	3.40
Fe 2p	710.77	5.00
C 1s	284.55	2.04

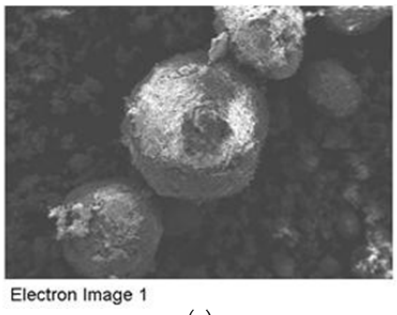

(a)

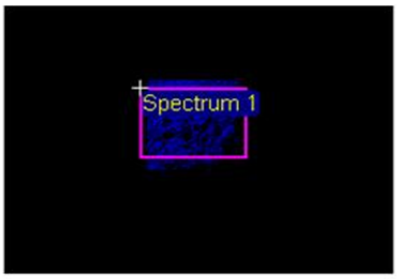

(b)

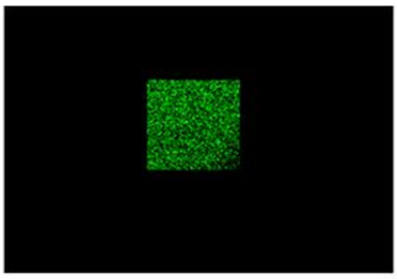

(c)

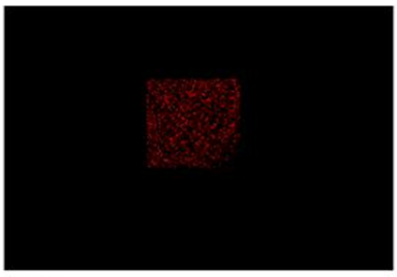

(d)

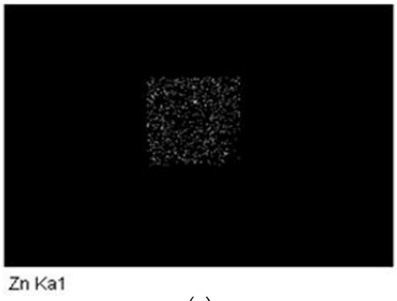

(e)

Fig. 5. SEM-EDX images of dispersed elements in LiNiZn-ferrite particle: (a) SEM image, (b) O, (c) Fe, (d) Ni, (e) Zn.

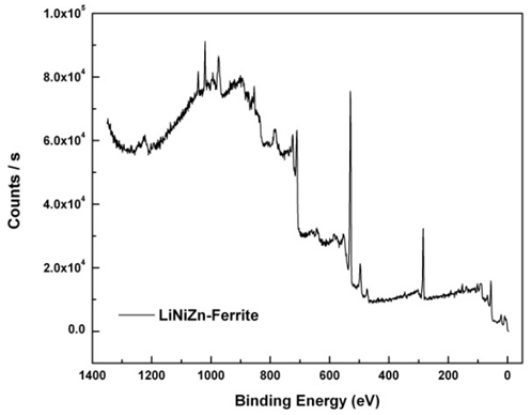

Fig. 6. XPS spectrum of elements on the surface of LiNiZn-ferrite.

of the Fe 2p peak is 5.00 eV. The Fe 2p peak consists of Fe_2O_3.

In Fig. 7(e), the Ni 2p peak position of nickel is approximately at 854.24 eV and the FWHM of the Ni 2p peak is 3.40 eV. The Ni 2p peak consists of NiO. In Fig. 7(f), the Zn 2p peak position of zinc is approximately at 1,020.29 eV and the FWHM of the Zn 2p peak is 3.33 eV. The Zn 2p peak consists of ZnO. It is determined that the XPS spectrums of elements are derived from oxide compounds and heat treatment. It is clear that LiNiZn-ferrite particles consist of lithium, iron, nickel, and zinc elements. When an EDX analysis was performed to analyze the elemental constituents on the surface of the sample, lithium could not be detected. However, it was possible to con-

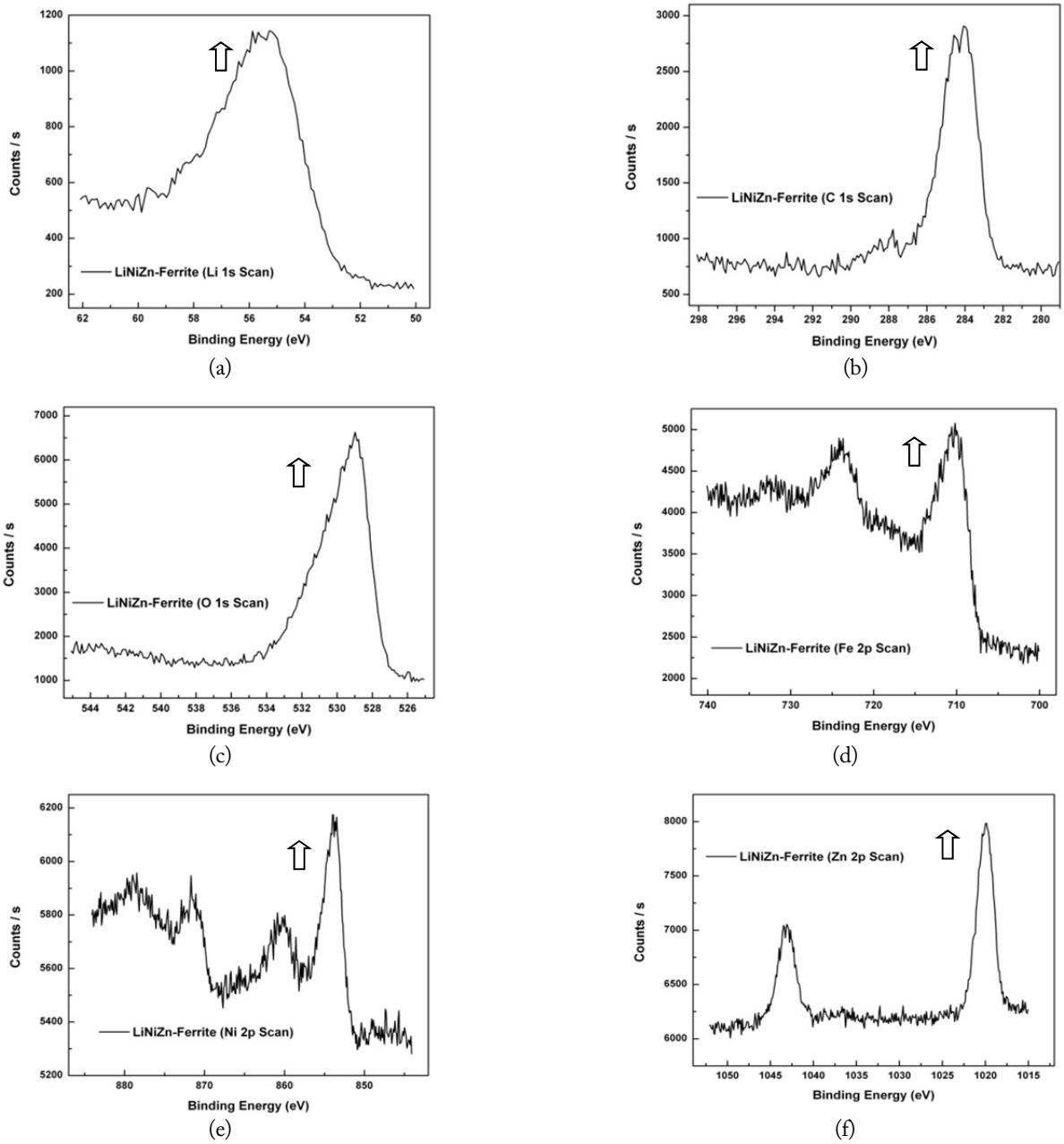

Fig. 7. XPS spectrums of Li 1s (a), C 1s (b), O 1s (c), Fe 2p (d), Ni 2p (e), and Zn 2p (f) on the surface of LiNiZn-ferrite.

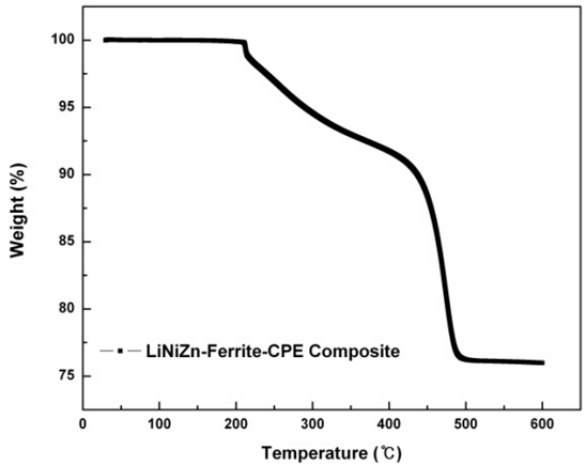

Fig. 8. TGA curve of LiNiZn-ferrite-CPE composite.

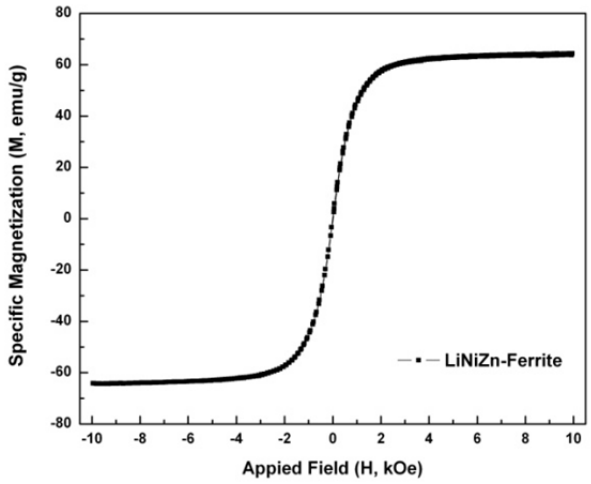

Fig. 9. Hysteresis curve of LiNiZn-ferrite.

firm lithium on the surface of the sample by detecting electron binding energy at XPS [25, 26].

As a piece of the toroid sample was heated, the variations in the weight percent of the sample were measured using TGA equipment. The TGA curve of the LiNiZn-ferrite-CPE composite is shown in Fig. 8. The weight loss percent versus temperature is up to 9% in the range of 200℃ to 420℃. The weight percent at the residue of the sample is up to 91%.

The corresponding part of the TGA curve shows a steep increase in the weight loss percent of up to 15% in the range of 420℃ to 500℃. The weight percent at the residue of the sample is up to 76%. The CPE is evaporated by heating up to 500 ℃. After 500℃, there is not significant weight loss. In Fig. 8, the weight percent ratio of LiNiZn-ferrite in the LiNiZn-ferrite-CPE composite can be expected to be approximately 76 % [19].

The application of a sufficiently large magnetic field causes the spins within a sample to align with the field. The maximum value of the magnetization achieved in this state is called the saturation magnetization (Ms). The Ms is 63.7 emu/g. As the magnitude of the magnetic field decreased, the spins cease to be aligned with the field and the total magnetization decreases. In ferromagnets, a residual magnetic moment remains at zero field. The value of the magnetization at zero field is called the remanent magnetization (Mr). The Mr is approximately 0.422 emu/g. The ratio of remanent magnetization to saturation magnetization (Mr/Ms) is called the remanence ratio and it varies from 0 to 1. Mr/Ms is approximately 0.007. The coercive field (Hc) is the magnitude of the field that must be applied in the negative direction to bring the magnetization of the sample back to zero. The coercive field is approximately −0.006 kOe. The magnetic properties of LiNiZn-ferrite were measured by VSM. The magnetic field reached up to 10 kOe. The hysteresis curve of LiNiZn-ferrite is shown in Fig. 9. The shape of the hysteresis curve is special interest for a soft magnetic material as an EM wave absorber, which requires a relatively large saturation magnetization and a relatively small coercivity [17, 20, 21].

The purpose of EM wave absorbers is a low reflection over a wide range of frequency. For certain applications, the EM wave absorbers should absorb incident plane waves over a wide frequency range and should be as thin as possible. The variations in the return loss versus frequency in the range of 10 MHz to 12 GHz were investigated by network analyzer. Fig. 10 and Table 3 show the obtained results in terms of the different limitative conditions [6, 7]. The positive return loss indicates the reflected power is small relative to the incident power. When the given condition of the return loss is over 3 dB and the thickness of the EM wave absorber is 2 mm, the absorption bandwidth is 5.11–11.10 GHz. When the thickness of the EM wave absorber is 4

Table 3. Obtained results in terms of the different limitative conditions for EM wave absorbing properties

Thickness (mm)	Center frequency (GHz)	Absorption bandwidth (GHz)					
		3 dB, 50%	5 dB, 68%	7 dB, 80%	10 dB, 90%	15 dB, 97%	20 dB, 99%
1	7.86	7.74–8.01	-	-	-	-	-
2	7.80	5.11–11.10	-	-	-	-	-
4	7.68	2.33–11.12	3.62–10.83	5.04–10.65	5.36–9.24	7.60–7.78	-
6	5.17	1.89–10.76	2.29–8.80	3.28–7.70	3.51–7.46	4.27–6.35	4.95–5.30
8	3.55	1.16–10.98	2.02–7.56	2.21–6.35	3.19–5.08	3.42–3.63	-

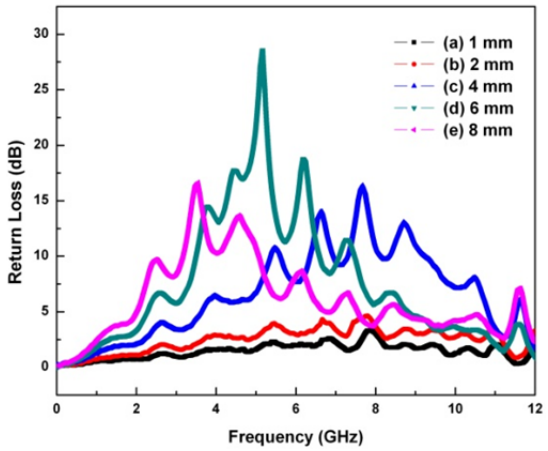

Fig. 10. Return losses of EM wave absorbers composed of LiNiZn-ferrite.

mm and the given condition of the return loss is over 3 dB, the absorption bandwidth is 2.33–11.12 GHz. In addition, when the given condition of the return loss is over 10 dB, the absorption bandwidth is 5.36–9.24 GHz. At the center frequency (7.68 GHz) of the EM wave absorber having a 4-mm thickness, the return loss is 16.35 dB. When the thickness of the EM wave absorber is 6 mm and the given condition of the return loss is over 3 dB, the absorption bandwidth is 1.89–10.76 GHz. In addition, when the given condition of the return loss is over 10 dB, the absorption bandwidth is 3.51–7.46 GHz. At the center frequency (5.17 GHz) of the EM wave absorber having a 6-mm thickness, the return loss is 28.58 dB. When the thickness of the EM wave absorber is 8 mm and the given condition of the return loss is over 3 dB, the absorption bandwidth is 1.16–10.98 GHz. In addition, when the given condition of the return loss is over 10 dB, the absorption bandwidth is 3.19–5.08 GHz. At the center frequency (3.55 GHz) of the EM wave absorber having an 8-mm thickness, the return loss is 16.65 dB. From Table 3, it can be found that the center frequency of the EM wave absorber shifts to a low frequency when the thickness of the EM wave absorber increases. A greater than 10 dB return loss is shown in the 4–8 mm thickness of the EM wave absorber, while it is not shown in the 1–2 mm thickness of the EM wave absorber. When the thickness of the EM wave absorber increases from 4 to 8 mm, the absorption bandwidth of a greater than 10 dB return loss shifts to a low frequency. The 10 dB return loss can be expressed as a 90% absorption ratio. As EM wave absorbers prevent false images on the screen of the radar, it is effective to apply EM wave absorbers having a greater than 10 dB return loss [27].

IV. Conclusion

In this study, we carried out experiments to demonstrate the dependence of thickness on the return loss of LiNiZn-ferrite-CPE composite. As an absorbent material, ferrite composite was composed of lithium, nickel, and zinc. LiNiZn-ferrite was prepared by the calcination and sintering method. We prepared CPE as a polymeric binder to make toroid samples. In SEM images of LiNiZn-ferrite particles, the appearances of particles are spherical in shape and the surfaces of particles are smooth. It is determined that the lithium oxide, nickel oxide, zinc oxide, and iron oxide particles were mixed and agglomerated to make LiNiZn-ferrite particles. EDX and XPS analyses were performed to analyze elemental constituents on the surface of the sample. It is determined that the EDX and XPS spectra of the elements are derived from oxide compounds and heat treatment. It is clear that LiNiZn-ferrite particles consist of lithium, iron, nickel, and zinc elements. As a piece of the toroid sample was heated, the variations in the weight percent of the sample were measured by TGA equipment. The weight percent ratio of LiNiZn-ferrite in the LiNiZn-ferrite-CPE composite can be expected to be approximately 76%. The hysteresis curve of the sample was measured by VSM. The saturation magnetization is 63.7 emu/g. The shape of the hysteresis curve is special interest for a soft magnetic material as an EM wave absorber, which requires a relatively large saturation magnetization and a relatively small coercivity. The variations in return loss versus frequency in the range of 10 MHz to 12 GHz were investigated by network analyzer. A greater than 10 dB return loss is shown in the 4–8 mm thickness of the EM wave absorber, while it is not shown in the 1–2 mm thickness of the EM wave absorber. When the thickness of the EM wave absorber increases from 4 to 8 mm, the absorption bandwidth of a greater than 10 dB return loss shifts to a low frequency. When the thickness of the EM wave absorber is 6 mm and the given condition of the return loss is greater than 10 dB, the absorption bandwidth is 3.51–7.46 GHz. At the center frequency (5.17 GHz) of the EM wave absorber having a 6-mm thickness, the return loss is 28.58 dB. The 10 dB return loss can be expressed as a 90% absorption ratio. As EM wave absorbers prevent false images on the radar screen, it is effective to apply EM wave absorbers having a greater than 10 dB return loss.

This research was partly supported by the Fuchs Lubricants (Korea) which is a Member of Fuchs Group/Germany, MA Electronic Company, and TODA Ferrite Korea.

References

[1] C. M. Choi and D. I. Kim, "A study on development of EM wave absorber using TiO_2 for automotive radar in cars," *Journal of the Korean Institute of Electromagnetic Engineering and Science*, vol. 8, no. 3, pp. 110-113, 2008.

[2] C. M. Choi, D. I. Kim, S. H. Je, and Y. S. Choi, "A study on

electromagnetic wave absorber for the collision-avoidance radar," *Current Applied Physics*, vol. 7, no. 5, pp. 586-589, 2007.

[3] S. M. Abbas, A. K. Dixit, R. Chatterjee, and T. C. Goel, "Complex permittivity and microwave absorption properties of $BaTiO_3$-polyaniline composite," *Materials Science and Engineering B*, vol. 123, no. 2, pp. 167-171, 2005.

[4] S. M. Abbas, A. K. Dixit, R. Chatterjee, and T. C. Goel, "Complex permittivity, complex permeability and microwave absorption properties of ferrite-polymer composites," *Journal of Magnetism and Magnetic Materials*, vol. 309, no. 1, pp. 20-24, 2007.

[5] K. Khan and S. Rehman, "Microwave absorbance properties of zirconium-manganese substituted cobalt nanoferrite as electromagnetic (EM) wave absorbers," *Materials Research Bulletin*, vol. 50, pp. 454-461, 2014.

[6] Y. B. Feng, T. Qiu, and C. Y. Shen, "Absorbing properties and structural design of microwave absorbers based on carbonyl iron and barium ferrite," *Journal of Magnetism and Magnetic Materials*, vol. 318, no. 1, pp. 8-13, 2007.

[7] W. Meng, D. Yuping, L. Shunhua, L. Xiaogang, and J. Zhijiang, "Absorption properties of carbonyl-iron/carbon black double-layer microwave absorbers," *Journal of Magnetism and Magnetic Materials*, vol. 321, no. 20, pp. 3442-3446, 2009.

[8] M. S. Kim, E. H. Min, and J. G. Koh, "Comparison of the effects of particle shape on thin FeSiCr electromagnetic wave absorber," *Journal of Magnetism and Magnetic Materials*, vol. 321, no. 6, pp. 581-585, 2009.

[9] S. M. Abbas, M. Chandra, A. Verma, R. Chatterjee, and T. C. Goel, "Complex permittivity and microwave absorption properties of a composite dielectric absorber," *Composites Part A: Applied Science and Manufacturing*, vol. 37, no. 11, pp. 2148-2154, 2006.

[10] C. H. Peng, C. C. Hwang, J. Wan, J. S. Tsai, and S. Y. Chen, "Microwave-absorbing characteristics for the composites of thermal-plastic polyurethane (TPU)-bonded NiZn-ferrites prepared by combustion synthesis method," *Materials Science and Engineering B*, vol. 117, no, 1, pp. 27-36, 2005.

[11] A. N. Yusoff and M. H. Abdullah, "Microwave electromagnetic and absorption properties of some LiZn ferrites," *Journal of Magnetism and Magnetic Materials*, vol. 269, no. 2, pp. 271-280, 2004.

[12] T. Nakamura, T. Miyamoto, and Y. Yamada, "Complex permeability spectra of polycrystalline Li-Zn ferrite and application to EM-wave absorber," *Journal of Magnetism and Magnetic Materials*, vol. 256, no. 1, pp. 340-347, 2003.

[13] Y. Hwang, "Microwave absorbing properties of NiZn-ferrite synthesized from waste iron oxide catalyst," *Materials Letters*, vol. 60, no. 27, pp. 3277-3280, 2006.

[14] R. Dosoudil, M. Usakova, J. Franek, J. Slama, and V. Olah, "RF electromagnetic wave absorbing properties of ferrite polymer composite materials," *Journal of Magnetism and Magnetic Materials*, vol. 304, no. 2, pp. e755-e757, 2006.

[15] S. G. Bachhav, R. S. Patil, P. B. Ahirrao, A. M. Patil, and D. R. Patil, "Microstructure and magnetic studies of Mg-Ni-Zn-Cu ferrites," *Materials Chemistry and Physics*, vol. 129, no. 3, pp. 1104-1109, 2011.

[16] A. C. F. M. Costa, A. P. Diniz, V. J. Silva, R. H. G. A. Kiminami, D. R. Cornejo, A. M. Gama, M. C. Rezende, and L. Gama, "Influence of calcinations temperature on the morphology and magnetic properties of Ni-Zn ferrite applied as an electromagnetic energy absorber," *Journal of Alloys and Compounds,* vol. 483, no. 1, pp. 563-565, 2009.

[17] W. Fu, S. Liu, W. Fan, H. Yang, X. Pang, J. Xu, and G. Zou, "Hollow glass microspheres coated with $CoFe_2O_4$ and its microwave absorption property, " *Journal of Magnetism and Magnetic Materials*, vol. 316, no. 1, pp. 54-58, 2007.

[18] F. Jin, H. Tong, J. Li, L. Shen, and P. K. Chu, "Structure and microwave-absorbing properties of Fe-particle containing alumina prepared by micro-arc discharge oxidation," *Surface & Coatings Technology*, vol. 201, no. 1, pp. 292-295, 2006.

[19] Y. Xie, X. Hong, J. Liu, Z. Le, F. Huang, Y. Qin, et al., "Synthesis and electromagnetic properties of $BaFe_{11.92}(LaNd)_{0.04}O_{19}$/titanium dioxide composites," *Material Research Bulletin*, vol. 50, pp. 483-489, 2014.

[20] B. F. Zou, T. D. Zhou, and J. Hu, "Effect of amorphous evolution on structure and absorption properties of FeSiCr alloy powder," *Journal of Magnetism and Magnetic Materials*, vol. 335, pp. 17-20, 2013.

[21] Y. Wang, F. Xu, L. Li, H. Liu, H. Qiu, and J. Jiang, "Magnetic properties of La-substituted Ni-Zn-Cr ferrite via rheological phase synthesis," *Materials Chemistry and Physics*, vol. 112, no. 3, pp. 769-773, 2008.

[22] T. G. Lee, J. B. Kim, and T. H. Noh, "Electromagnetic wave absorption characteristics of nanocrystalline FeCuNbSiB alloy flakes/polymer composite sheets with different flake thickness," *Journal of Magnetics*, vol. 14, no. 4, pp. 155-160, 2009.

[23] X. G. Liu, B. Li, D. Y. Geng, W. B. Cui, F. Yang, Z. G. Xie, D. J. Kang, and Z. D. Zhang, "(Fe, Ni)/C nanocapsules for electromagnetic wave absorber in the whole Ku-band," *Carbon*, vol. 47, no. 2, pp. 470-474, 2009.

[24] M. K. Tehrani, A. Ghasemi, M. Moradi, and R. S. Alam, "Wideband electromagnetic wave absorber using doped barium hexaferrite in Ku-band," *Journal of Alloys and Compounds*, vol. 509, no. 33, pp. 8398-8400, 2011.

[25] A. P. Grosvenor, M. C. Biesinger, R. C. Smart, and N. S. McIntyre, "New interpretations of XPS spectra of nickel

metal and oxides," *Surface Science*, vol. 600, no. 9, pp. 1771-1779, 2006.
[26] T. Yamashita and P. Hayes, "Analysis of XPS spectra of Fe^{2+} and Fe^{3+} ions in oxide materials," *Applied Surface Science*, vol. 254, no. 8, pp. 2441-2449, 2008.
[27] M. S. Lin, C. G. Hsu, C. H. Chiang, and C. K. Cho, "Measurement and analysis techniques for designing microwave absorbers," *Journal of Chung Cheng Institute of Technology*, vol. 43, no. 2, pp. 29-39, 2014.

Dong-Young Kim

received a B.S. degree in Electric Electronic Engineering from Hanyang University, Korea in 2008. He worked as an Engineer on the Engineering Team at DongWoo Fine-Chem, which belongs to Sumitomo Chemical Group in Japan. He is currently working as a researcher in the Naval Ship Department, Defense Agency for Technology and Quality, Korea. His research interests include Electromagnetic Wave Absorbing Material, Electrode Material, Organic Chemistry, Python, Machine Learning, and Economic Mathematics.

Young-Ho Yoon

received B.S. and M.S. degrees in Electronics Engineering from Kyungpook National University, Daegu, Korea, in 1996 and 1999, respectively. He is currently working as a senior researcher at Defense Agency for Technology and Quality, Korea. His research interests include RF Filters and Electric Equipment Systems in Naval Ships.

Kwan-Jun Jo

received B.S. and M.S. and Ph.D. degrees in Mechatronics Engineering from Korea Maritime University, Busan, Korea in 2005, 2007, and 2012, respectively. He is currently working as a senior researcher in the Defense Reliability Program Department, Defense Agency for Technology and Quality, Korea. His research interests include Signal Filtering, Quality Management, and Reliability Engineering.

Gil-Bong Jung

received a Ph.D. in Material Science of Engineering from Changwon National University, Korea in 2010. He is currently working as principal researcher in the Localization Program Management Department at Defense Agency for Technology and Quality. His research interests include Coating Material of Electromagnetic Wave Absorbing Property.

Chong-Chul An

received a B.S. degree in Chemical Engineering from Chonnam National University, Korea in 1989. He worked as a researcher to research magnetic material at Korea Institute of Science and Technology (KIST). He is currently working as a CEO at MA Electronic Co. His research interests include Electromagnetic Wave Absorber and Magnetic Material.